1996ApJ...465..840S

THE ASTROPHYSICAL JOURNAL, 465:840–844, 1996 July 10
© 1996. The American Astronomical Society. All rights reserved. Printed in U.S.A.

A STUDY OF THE EVOLUTIONARY STATE OF THE SUPERNOVA REMNANT G299.2−2.9

PATRICK SLANE, OLAF VANCURA, AND JOHN P. HUGHES
Harvard-Smithsonian Center for Astrophysics, 60 Garden Street, Cambridge, MA 02138; slane@cfa.harvard.edu; ov@cfa.harvard.edu; jph@cfa.harvard.edu
Received 1995 September 29; accepted 1996 January 26

ABSTRACT

Using archival data from the *Einstein* Slew Survey (ESS) and the *Infrared Astronomical Satellite* (*IRAS*), as well as results from the *ROSAT* All-Sky Survey (Busser et al.), we present an investigation of the newly discovered supernova remnant (SNR) G299.2−2.9. The object appears morphologically similar in the IR and X-ray bands, with a partially complete shell that is brightest in the northeast. The radio morphology is also similar, although a bright region in the western portion of the remnant is also evident. Results reported from the *ROSAT* Position Sensitive Proportional Counter (PSPC) observation include a low value for the line-of-sight interstellar column density, suggestive of a nearby remnant (distance ∼0.5 kpc), leading Busser et al. to conclude G299.2−2.9 is a young remnant that has not yet entered the adiabatic stage of evolution. We investigate the properties expected from such a scenario and find that the results imply an extremely underluminous SNR. As an alternative, we consider an interpretation whereby the SNR is at a larger distance and in the Sedov phase of evolution. Using a model for a nonradiative shock propagating through a dusty interstellar medium, we show that a self-consistent model can reproduce the X-ray and IR fluxes. We discuss the plausibility of each of these models and propose observational tests to differentiate between the two scenarios.

Subject headings: ISM: individual (G299.2−2.9) — supernova remnants — X-rays: ISM

1. INTRODUCTION

Supernovae (SNe) are believed to result from either the core collapse of a massive star (Type II/Ib, c SN) or the thermonuclear explosion of an accreting white dwarf (Type Ia SN). Observations of SNe near maximum brightness show that these events involve the ejection of stellar material with kinetic energies in the range $\sim 10^{50}$–10^{51} ergs. Although the uncertainties in the determination of this quantity for any individual SN are large, there does not appear to be any strong evidence for a correlation between SN type and explosion energy, which may be surprising given the very different explosion mechanisms and range of possible progenitors involved. As SNe evolve into remnants by sweeping up the ambient circumstellar or interstellar medium (ISM), much of the ejecta's kinetic energy gets converted into the thermal energy content of the shock-heated ISM. Thus, studies of the energetics, thermodynamic state, and evolutionary state of supernova remnants (SNRs) can provide critical information about the initial explosion energies of SNe. In this paper, we study the evolutionary state of a recently discovered SNR, G299.2−2.9, to determine whether the data on the remnant fits within this established scenario or whether it indicates the need for a hitherto unrecognized new class of subluminous remnants of subenergetic supernova explosions.

2. OBSERVATIONS

First discovered as the extended source 1ES 1212−651 in the *Einstein* Slew Survey (ESS) data (Elvis et al. 1992), G299.2−2.9 is a recently identified SNR (Busser et al. 1995a, b) in the *ROSAT* All-Sky Survey (RASS) data (Snowden & Schmitt 1990). The remnant is relatively bright (3.2 counts s^{-1} in the PSPC) with a diameter of ∼15′. The Position Sensitive Proportional Counter (PSPC) spectral data also suggest a temperature $T \sim 8 \times 10^6$ K with a neutral hydrogen column density $N_H \sim 3 \times 10^{20}$ cm^{-2}, yielding an unabsorbed flux $F_x \sim 3.3 \times 10^{-11}$ ergs cm^{-2} s^{-1}. Based upon the derived N_H value, Busser et al. (1995a, b) estimate a source distance $d \approx 0.5$ kpc assuming a mean ISM number density of $\bar{n} = 0.2$ cm^{-3}. At this distance, the luminosity is $L_x \sim 1 \times 10^{33}$ ergs s^{-1}, and the radius of the remnant is $R \sim 1.1$ pc. We note, however, that the RASS exposure of ∼220 s (Busser et al. 1995b) leads to considerable uncertainty in the derived spectral parameters; a considerably larger column density, for example, is not ruled out at the 2–3 σ level.

The ESS image of the remnant is illustrated in Figure 1, where we have smoothed the data with a 1′ Gaussian. While limited to only ∼55 counts in the 33 s effective exposure, the remnant morphology appears to be that of an incomplete shell with the brightest emission concentrated in the east. Busser et al. (1995a) report a centrally brightened morphology, in apparent conflict with Figure 1. We note that the emission from this region was identified as two distinct sources in the ESS (see Table 1): 1ES 1212−651 (the northern region) was classified as an unidentified extended source, while 1ES 1212−652 (the southern region located ∼6′ away) was identified as a point source. Using a circle of radius 7′.5 to extract counts, we find an IPC count rate of 1.4 s^{-1}, in excellent agreement with the PSPC rate given the derived spectral parameters.

A column density $N_H = 3 \times 10^{20}$ cm^{-2} implies optical extinction $E_{B-V} = 0.05$ (Gorenstein 1975), suggesting that any optical emission from the remnant should be readily observable. Indeed, the ESO/SRC red survey plates show faint filaments around the southern rim of G299.2−2.9, with emission in the western and central regions as well (see Fig. 1). Busser et al. (1995b) report emission of [S II] and [O III], which is typically associated with the recombination zone of radiative shocks.

A ring of emission is also evident in the *IRAS* data. Figure 2 is a map showing the ratio of 60 μm to 100 μm flux that illustrates the infrared emission, presumably associated

© American Astronomical Society • Provided by the NASA Astrophysics Data System

1996ApJ...465..840S

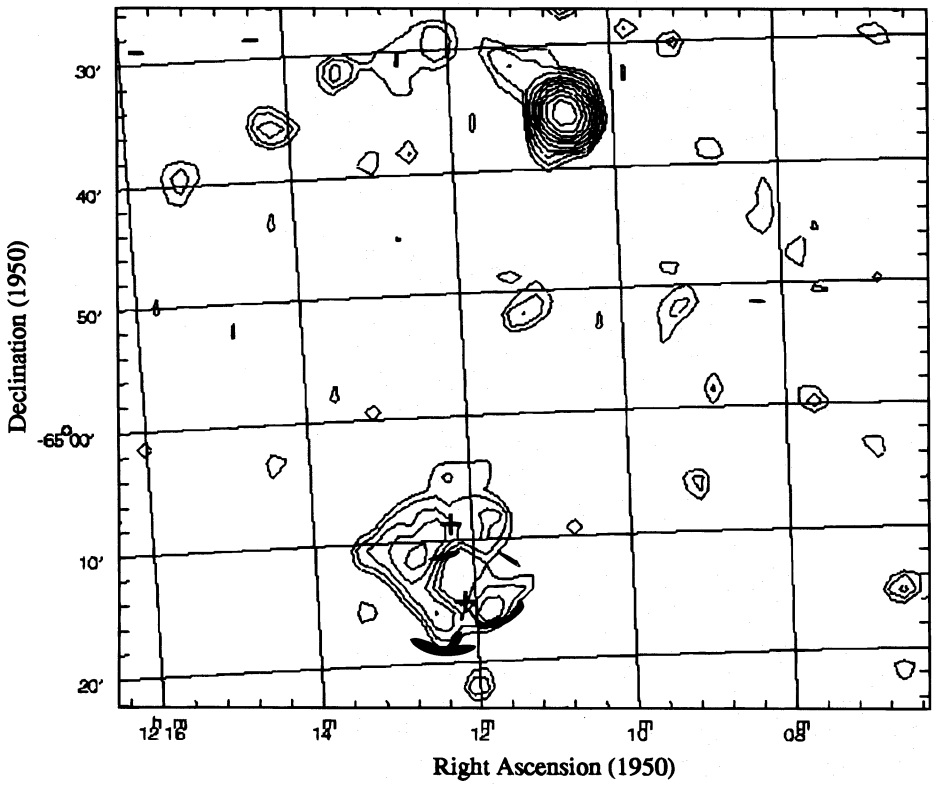

FIG. 1.—ESS image of G299.2 – 2.9 (*lower*). The morphology is suggestive of a shellike remnant, although counting statistics are limited. Optical emission as seen in the ESO/SRC red survey plates is indicated schematically as darkened regions on the image. Positions of the two 1ES sources (see Table 1) are indicated with crosses.

with shock heating of the surrounding dust. The infrared morphology appears remarkably similar to that in Figure 1 with respect to overall size, the presence of strong limb brightening, and the enhanced emission in the northeast. Using the SNR profile evident in the ratio map as a template, we have determined the 60 and 100 μm fluxes for G299.2 – 2.9 from the *IRAS* sky survey data (see Saken, Fesen, & Shull 1992). Background was estimated from the regions immediately surrounding the remnant in an effort to minimize the effects of large-scale variations in the background level. The derived fluxes are $F_{60} \approx 9.5$ Jy and $F_{100} \approx 2.3$ Jy, which are comparable to the lowest values quoted by Saken et al. (1992) for any remnant in their sample. The absolute calibration uncertainties for *IRAS* are of order 20% or larger (Saken et al. 1992). However, the flux values we derive are additionally uncertain due to the sensitivity to the exact size of the source and background regions. We estimate the uncertainty in the 60 and 100 μm flux values to be $\sim$35% and $\sim$60%, respectively.

Finally, two distinct radio sources coincident with the extended regions of G299.2 – 2.9 are listed in the PMN 4.85 GHz radio survey catalog (Wright et al. 1994), with a combined flux of $\sim$180 mJy. The survey image (Fig. 3) clearly shows associated diffuse emission as well, very similar to the shell-like X-ray and IR morphology, except for particularly enhanced emission in the western region of the remnant. The integrated flux for the remnant is $F_{4.85} \sim 340$ mJy. Based upon the uncertainties quoted for the point sources, we estimate $\sim$15% uncertainty in the SNR flux.

TABLE 1

ESS/RASS SOURCE COORDINATES

SOURCE	POSITION (1950) R.A.	POSITION (1950) Decl.	POSITION (2000) R.A.	POSITION (2000) Decl.
1ES 1212 – 652.....	$12^h12^m04^s$	−65°15′39″	$12^h14^m46^s$	−65°32′20″
1ES 1212 – 651.....	12 12 29	−65 09 30	12 15 12	−65 26 11
G299.2 – 2.9.....	12 12 29	−65 13 23	12 15 12	−65 30 04

3. INTERPRETATION

3.1. *X-Ray Properties of* G299.2 – 2.9

The proton density of the X-ray–emitting material is given by

$$n = \left(\frac{4\pi d^2 F_x}{V\Lambda_x}\right)^{1/2}, \quad (1)$$

where Λ_x is the intrinsic 0.1–2.4 keV band X-ray emissivity for a unit parcel of hot plasma at unit density. For the parameters given above, and assuming $\Lambda_x = 5 \times 10^{-23}$ ergs s^{-1} cm^3 (see further discussion below) along with a simple shell geometry, we find $n \approx 0.7\, d_{0.5}^{-1/2}$ cm^{-3}. Here $d_{0.5}$ is the distance to the remnant in units of 0.5 kpc. Assuming a preshock density $n_0 = n/4$, the mass swept up by the remnant is then $M_{sw} \approx 2.4 \times 10^{-2}\, d_{0.5}^{5/2}\, M_\odot$. If $d_{0.5} = 1$, such a small swept-up component implies that the remnant has not yet entered the Sedov phase (Sedov 1959) and that the X-ray emission should be dominated by the supernova ejecta.

We may also estimate the thermal energy content of the remnant. If we assume electron-ion equilibration, and

© American Astronomical Society • Provided by the NASA Astrophysics Data System

1996ApJ...465..840S

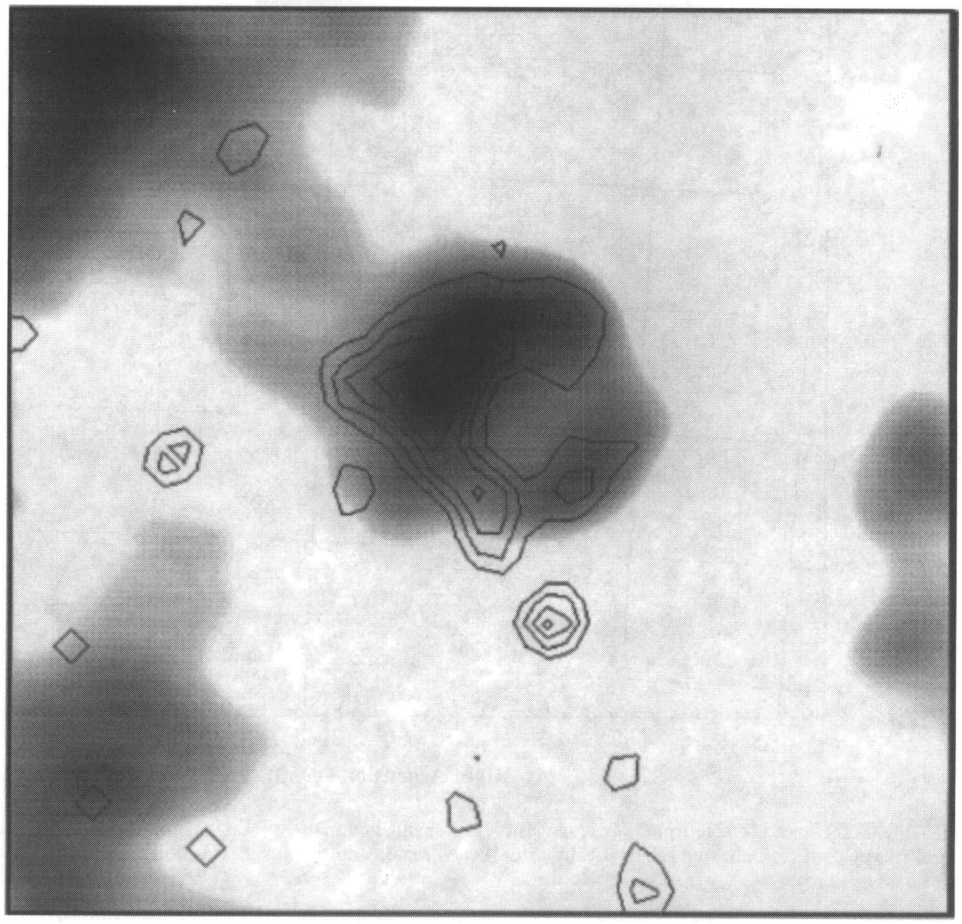

FIG. 2.—*IRAS* image of G299.2−2.9 showing ratio of 60 μm to 100 μm flux with X-ray contours from ESS image. The *IRAS* image has been smoothed with a ∼1′ Gaussian. Evidence for shock-heated dust emission associated with G299.2−2.9 is clearly seen, with a morphology similar to that observed in X-rays.

$n = 0.7\ \mathrm{cm}^{-3}$, then

$$E_{\mathrm{th}} = \frac{3}{2} NkT \approx 5 \times 10^{46}\, d_{0.5}^{2.5}\ \mathrm{ergs}\ . \qquad (2)$$

Typically, the thermal contribution represents ∼70% of the total explosion energy for a remnant in the Sedov phase of evolution (Cox & Franco 1981), thus implying a severely underenergetic remnant. If Coulomb equilibration timescales are assumed to be long compared with the remnant age, the associated ion temperature could be considerably (up to a factor of 100) larger, but, even in this case, the energy would still be remarkably low. For comparison, the thermal energy for the young ($t \approx 2000$ yr) oxygen-rich remnant G299.0+1.8 is $\sim 10^{50}$ ergs assuming electron-ion temperature equilibration (Hughes & Singh 1994).

3.2. *Evolutionary Scenarios*

We have considered two distinct scenarios for G299.2−2.9 in an attempt to arrive at a self-consistent interpretation of the observations: a nearby young remnant and a distant Sedov-phase remnant. The two scenarios lead to distinct observational properties that can be differentiated with future observations.

3.2.1. *Young Remnant*

If the distance to G299.2−2.9 is indeed small, as implied by the low–X-ray absorption, then the remnant is extremely young. Since, during the free expansion phase, the SNR expands more rapidly than in the adiabatic (Sedov) phase, we may derive an upper limit to the SNR age, t (in years), from the Sedov solution

$$t = 466 R \left(\frac{T_s}{10^7\ \mathrm{K}} \right)^{-1/2}\ , \qquad (3)$$

where R is the remnant radius in parsecs and T_s is the shock temperature. This yields an age $t \approx 560\, d_{0.5}$ yr. Here we have assumed that the measured electron temperature (corrected for emission-measure weighting assuming a Sedov profile) corresponds to the post–blast-wave gas in temperature equilibrium. If the electrons and ions have not yet equilibrated, then the blast-wave velocity will be greater than we have assumed, leading to an even younger remnant. On the other hand, if the observed emission is actually associated with the ejecta, then the observed temperature is that of the reverse shock. The blast-wave temperature (and thus velocity) would be larger still, and the age correspondingly smaller. Finally, the free-expansion age is $360\, d_{0.5}$ yr assuming an undecelerated velocity of the ejecta of 3×10^3 km s^{-1}. The lack of any historical reference to the associated supernova explosion raises serious doubts about such a small derived age, although the large southern declination of the remnant could plausibly account for this.

As shown above, at a distance of 0.5 kpc the thermal energy contained in the remnant is considerably smaller

© American Astronomical Society • Provided by the NASA Astrophysics Data System

1996ApJ...465..840S

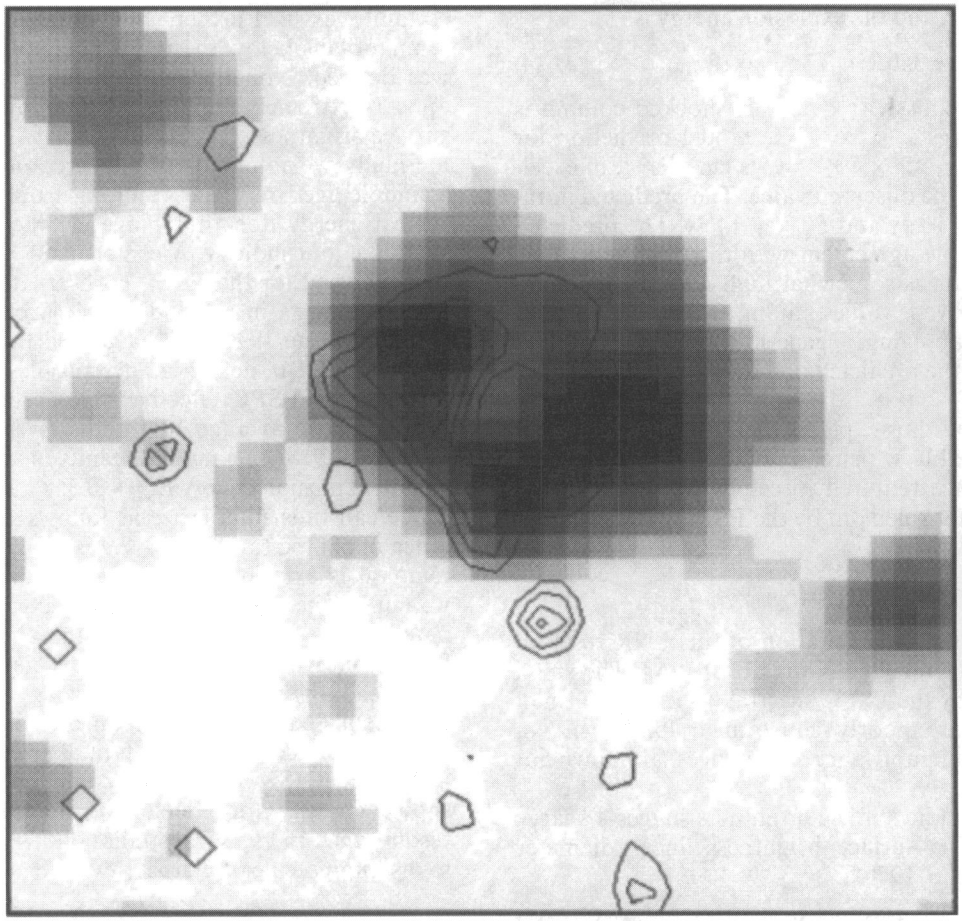

FIG. 3.—4.85 GHz image of G299.2 − 2.9 (from PMN survey) with X-ray contours from ESS image. The morphology is similar to that observed in X-rays and IR.

than the 10^{50}–10^{51} ergs typically associated with a supernova explosion. While such an underluminous explosion could perhaps explain the lack of a historical record, it would appear more plausible that the distance to the remnant has been underestimated.

We note that the spectral characteristics of a remnant in such an early phase of evolution would be unmistakable; like the emission from other very young remnants (e.g., Tycho or Cas A), the emission in the *Einstein*/*ROSAT* X-ray band should be dominated by that from the shocked ejecta component as opposed to the swept-up ambient ISM. In the optical, the remnant may show faint nonradiative Balmer emission (cf. Tycho, SN 1006) or bright clumpy emission with enriched abundances (cf. Cas A, Kepler).

3.2.2. *Sedov-Phase Remnant*

We can relax the problems with the age and energetics described above if the distance to the remnant has been underestimated. We find that, for a distance $d = 5$ kpc, a Sedov model for the remnant leads to reasonable values for the age and the explosion energy, and predicts roughly the correct flux for both the X-ray and infrared emission.

We have investigated the IR and X-ray characteristics of the remnant assuming different distances by using the nonradiative shock wave models of Vancura et al. (1994), which incorporate the effects of grain destruction and heating on the emission of the postshock gas. For a given preshock density and shock velocity, the model predicts X-ray and IR fluxes, and electron temperature assuming Coulomb equilibration, as a function of shocked column density. We note that, although these models assume steady state shocks and ignore the deceleration of the blast wave, they can be used to estimate the X-ray and IR emissions (see discussion in Vancura et al. 1994).

The larger assumed distance implies a larger $N_{\rm H}$ value as well, which, in turn, leads to different derived spectral values. To estimate this effect, we generated a simulated PSPC spectrum based upon the results reported by Busser et al. (1995b) and then fitted the spectrum to a single-temperature thermal plasma model (Raymond 1979) with $N_{\rm H}$ scaled by the ratio of the distances. For each distance considered, we determined n_0 from equation (1), assuming a Sedov geometry. We then used the model to determine the shock velocity required for the electron temperature to match the observed value when the shocked column reached that implied by n_0 and the remnant size at this distance. The predicted X-ray flux was then compared with that observed.

We find that a distance of ~ 5 kpc yields a self-consistent solution. For this distance, the estimated spectral values of $T = 6.0 \times 10^6$ K and $F_x = 9.2 \times 10^{-11}$ ergs cm^{-2} s^{-1} lead to a preshock density of $n_0 = 9.3 \times 10^{-2}$ cm^{-3}. With a radius of 11 pc, the total shocked column is thus $N_s = 3.1 \times 10^{18}$ cm^{-2}. We find that a shock velocity $v_s \sim 700$ km s^{-1} is required for the electron temperature to match the derived temperature at this value for N_s. The remnant age is

© American Astronomical Society • Provided by the NASA Astrophysics Data System

1996ApJ...465..840S

then $t \approx 6.6 \times 10^3$ yr, and the explosion energy is

$$E_{51} \approx 340 R^5 n_0 t^{-2} = 0.12 . \quad (4)$$

The average X-ray emissivity over this shocked column is $\Lambda_x = 4.6 \times 10^{-23}$ ergs s^{-1} cm^3. The model prediction for the X-ray flux is $F_x = 9.1 \times 10^{-11}$ ergs cm^{-2} s^{-1}, in excellent agreement with the observed value. The predicted infrared fluxes are $F_{60} = 16$ Jy and $F_{100} = 14$ Jy. The predicted 60 μm is in reasonable agreement with the observed value, while that for 100 μm is somewhat high. Given the uncertainties in the derived values, along with the approximations made in applying a generic model, the level of agreement between the predicted and observed values is not unreasonable.

This interpretation thus explains the observed characteristics quite comfortably with reasonable SNR parameters, although the distance required forces us to adopt an N_H value that, though not ruled out by the PSPC data, is higher than the best-fit value.

4. DISCUSSION

Clearly much of the interpretation of this SNR rests on the distance inferred from the X-ray absorption. The small N_H value preferred by the PSPC spectral fits implies a small distance. The fits are poorly constrained for large N_H, however, and considerably larger distances are thus not ruled out.

We note that the radio surface brightness suggests a large distance as well. The surface brightness–linear diameter (Σ-D) relation of Milne (1979),

$$\Sigma_{1\,\mathrm{GHz}} = 3.4 \times 10^{-15} D^{-3.8} \text{ W m}^{-2} \text{ Hz}^{-1} \text{ sr}^{-1} , \quad (5)$$

predicts a distance $d \sim 16$–21 kpc for spectral indices between 0.9 and 0.2. While our X-ray/IR analysis does not rule out such a large distance, problems with deriving distances from the empirical Σ-D relation are well documented (e.g., Green 1984); uncertainties as large as factors of 2–4 certainly exist. Further, the surface brightness for this remnant falls below the range over which the Σ-D relation was derived. Nonetheless, a distance as small as 0.5 kpc appears extremely unlikely, based upon the observed radio surface brightness.

Finally, we note that our interpretation of G299.2−2.9 as a middle-aged remnant resulting from a SN explosion of typical energy does not hinge on the interpretation of a shell-like morphology. A center-filled X-ray profile such as that reported for the *ROSAT* observations can result from SNR evolution in a cloudy ISM (McKee & Cowie 1977; White & Long 1991). We have used the model of White & Long (1991) to derive model profiles that, when folded through the PSPC effective area, produce a center-filled profile whose average brightness is the same as that for G299.2−2.9. Such a models results in an age $t \sim 5 \times 10^3$ yr and an explosion energy $E_{51} \sim 0.3$.

We can thus summarize as follows. If the estimated distance of 500 pc to G299.2−2.9 is roughly correct, then the remnant is extremely young and the associated explosion was underenergetic. The X-ray spectrum should be dominated by ejecta contributions, and the optical spectra, if from radiative shocks, should show ejecta-like abundances. If, instead, the distance is $\sim$5 kpc, as suggested by the self-consistent Sedov interpretation described above, then the emission will contain a substantial swept-up component of the ambient ISM. Both X-ray and optical spectra should show cosmic (or depleted) abundances. Moderate-resolution X-ray spectral studies of this remnant will be able to discriminate between these two scenarios.

The authors would like to thank David Helfand for his careful review of this paper and, in particular, for bringing the radio data to our attention. This work was supported in part by the National Aeronautics and Space Administration through contract NAS 8-39073, and grants NAG 5-2368, NAG 5-2453, and NAG 5-2565.

REFERENCES

Busser, J.-U., Egger, R. J., & Aschenbach, B. 1995a, IAU Circ., No. 6142
———. 1995b, in Proc. Röntgenstrahlung from the Universe: An International Conference on X-Ray Astronomy and Astrophysics, in press
Cox, D. P., & Franco, F. 1981, ApJ, 251, 687
Elvis, M., Plummer, D., Schachter, J., & Fabbiano, G. 1992, ApJS, 80, 257
Gorenstein, P. 1975, ApJ, 198, 40
Green, D. A. 1984, MNRAS, 209, 449
Hughes, J. P., & Singh, K.-P. 1994, ApJ, 422, 126
McKee, C. F., & Cowie, L. L. 1977, ApJ, 215, 213
Milne, D. K. 1979, Australian J. Phys., 32, 83
Raymond, J. C. 1979, ApJS, 39, 1
Saken, J. M., Fesen, R. A., & Shull, J. M. 1992, ApJS, 81, 715
Sedov, L. I. 1959, Similarity and Dimensional Methods in Mechanics (New York: Academic)
Snowden, S. L., & Schmitt, J. H. M. M. 1990, Ap&SS, 171, 207
Vancura, O., Raymond, J. C., Dwek, E., Blair, W. P., Long, K. S., & Foster, S. 1994, ApJ, 431, 188
White, R. L., & Long, K. S. 1991, ApJ, 373, 543
Wright, A. E., Griffith, M. R., Burke, B. F., & Ekers, R. D. 1994, ApJS, 91, 111

© American Astronomical Society • Provided by the NASA Astrophysics Data System